

## Dynamics of Be-Star Decretion Disks in Be/X-ray Binaries

A. T. Okazaki

*Faculty of Engineering, Hokkai-Gakuen University, Toyohira-ku,  
Sapporo 062-8605, Japan*

**Abstract.** We study the dynamics of the viscous decretion disk around the Be star in Be/X-ray binaries, based on the results from three dimensional SPH simulations. We find that the Be disk is tidally truncated at a radius smaller than the periastron distance, except in systems with very high orbital eccentricity and/or large inclination angles. Owing to the tidal effect by the neutron star in an eccentric orbit, the structure of the Be disk varies with the orbital phase. We show how the H $\alpha$  line profile varies with the variation in the disk structure.

### 1. Introduction

Recent study of Be stars has established that the Be disk is nearly Keplerian. A natural mechanism to form a nearly Keplerian disk around a star is the viscous decretion, which was proposed by Lee, Saio, & Osaki (1991) and has been shown to explain many of the observed features. According to this scenario, the matter supplied from the equatorial surface of the star drifts outwards because of the viscous effect and forms the disc.

The Be/X-ray binaries represent the largest subclass of high-mass X-ray binaries and consist of a Be star and a neutron star. They have wide (several tens of days  $\lesssim P_{\text{orb}} \lesssim$  several hundred days) and mostly eccentric ( $e \gtrsim 0.3$ ) orbits. Based on the viscous decretion disk model, Negueruela & Okazaki (2001) and Okazaki & Negueruela (2001) semi-analytically showed that the coplanar Be disk in Be/X-ray binaries is truncated at a radius smaller than the periastron distance, as long as  $\alpha_{\text{SS}} \ll 1$ , where  $\alpha_{\text{SS}}$  is the Shakura-Sunyaev viscosity parameter. The result agrees with the observations (Reig, Fabregat, & Coe 1997; Zamanov et al. 2001) and has been confirmed by numerical simulations (Okazaki et al. 2002).

In this paper, we explore the dynamics of Be disks in Be/X-ray binaries, using 3D SPH simulations for a wider range of orbital parameters.

### 2. Numerical Model

We use a 3D SPH code, in which the Be disk is modeled by an ensemble of gas particles of negligible masses and the Be star and the neutron star by two sink particles with corresponding masses (Okazaki et al. 2002; see also Bate, Bonnell, & Price 1995). For simplicity, we assume that the disk is isothermal at the temperature of half the effective temperature of the Be star and has the viscosity parameter  $\alpha_{\text{SS}} = 0.1$ . We also assume that the neutron star has a variable accretion radius depending on the instantaneous binary separation.

The mass ejection mechanism from the Be star is modeled by constant injection of gas particles at a radius just outside the equatorial surface. As the Be star, we take a B0V star of  $M_* = 18M_\odot$ ,  $R_* = 8R_\odot$ , and  $T_{\text{eff}} = 26,000$  K.

### 3. Evolution of the Be Disk in Coplanar Systems

Figure 1 shows the surface density evolution for short-period ( $P_{\text{orb}} = 24.3$  d) systems with different eccentricity  $e$ . We have found that the Be disk is resonantly truncated at a radius smaller than the periastron distance, except for systems with extremely high orbital eccentricity ( $e \gtrsim 0.8$ ). The truncation is most efficient for the circular binary and becomes less efficient for higher eccentricity.

For comparison, the surface density evolution for long-period ( $P_{\text{orb}} = 100$  d) systems is shown in Figure 2. Note that the efficiency of tidal/resonant truncation is weaker for a longer orbital period.

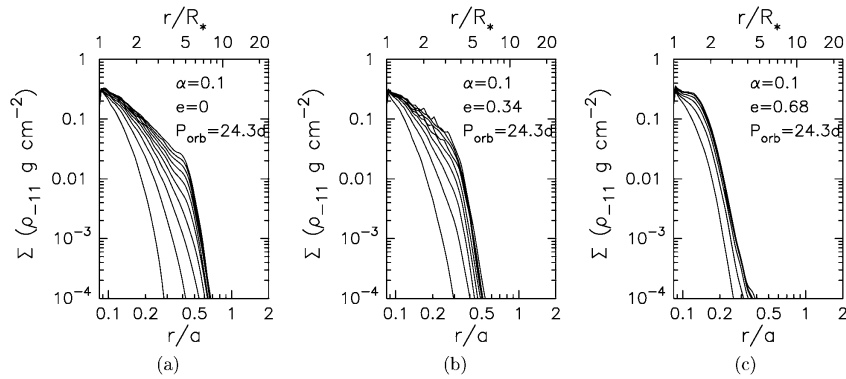


Figure 1. Surface density evolution of the Be decretion disk for  $P_{\text{orb}} = 24.3$  d: (a)  $e = 0$ , (b)  $e = 0.34$ , and (c)  $e = 0.68$ . The time interval between adjacent contours is  $5P_{\text{orb}}$ .  $\rho_{-11} = \rho_0/10^{-11} \text{ g cm}^{-3}$ , where  $\rho_0$  is the base density of the disk.

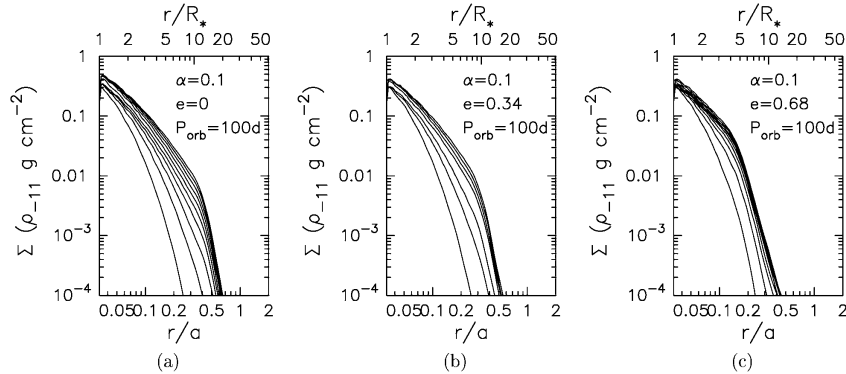


Figure 2. Same as Figure 1, but for  $P_{\text{orb}} = 100$  d.

#### 4. Evolution of the Be Disk in Misaligned Systems

Figure 3 shows the surface density evolution in misaligned systems with  $P_{\text{orb}} = 24.3$  d and  $e = 0.34$ . It should be noted that the tidal/resonant truncation works for misaligned systems as it does for coplanar ones. The truncation, however, is less efficient for a higher inclination angle  $i$ . Little truncation is seen for  $i > 60^\circ$ .

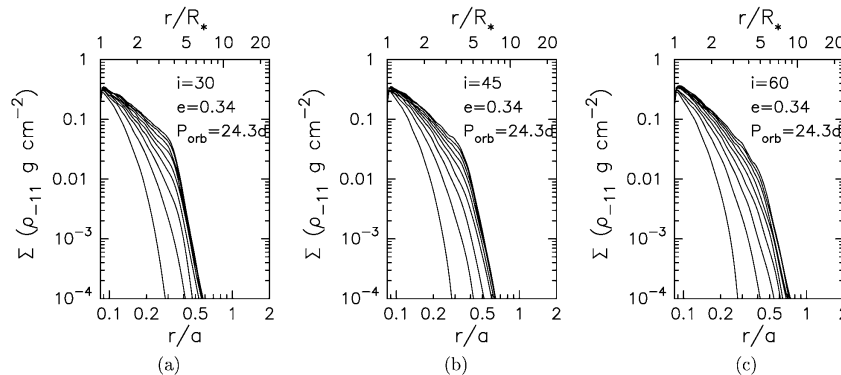


Figure 3. Surface density evolution of the Be accretion disk for  $P_{\text{orb}} = 24.3$  d and  $e = 0.34$ : (a)  $i = 30^\circ$ , (b)  $i = 45^\circ$ , and (c)  $i = 60^\circ$ . The initial azimuth of the tilt is set toward the periastron. The format of the figure is the same as that of Figure 1

#### 5. Phase Dependence of H $\alpha$ Line Profiles

Figure 4 gives snapshots covering one orbital period for  $P_{\text{orb}} = 24.3$  d,  $e = 0.34$ , and  $i = 0$ . The spiral density wave is clearly seen between the periastron passage and the apastron passage.

In order to see whether the disturbance in the Be disk caused by the neutron star gives an observable effect on the emission line profiles, we have calculated the H $\alpha$  line profiles from the Be disk, using the simulation data shown in Figure 4 and the method described in Okazaki (1996). The left panel of Figure 5 presents the dynamical spectrum for one orbital period, in which the variation after the periastron passage at  $t/P_{\text{orb}} = 46.5$  is clearly seen. As shown in the upper right panel of Figure 5, the separation of the double peaks of the H $\alpha$  line oscillates as the density wave rotates. The equivalent width shows little orbital modulation for this moderate value of eccentricity  $e = 0.34$  (see the lower right panel).

#### References

- Bate, M. R., Bonnell, I. A., & Price, N. M. 1995, MNRAS, 285, 33  
 Lee, U., Saio, H., & Osaki, Y. 1991, MNRAS, 250, 432  
 Negueruela, I. & Okazaki, A. T. 2001, A&A, 369, 108  
 Okazaki, A. T. 1996, PASJ, 48, 305  
 Okazaki, A. T. 2001, PASJ, 53, 119  
 Okazaki, A. T. & Negueruela, I. 2001, A&A, 377, 161  
 Okazaki, A. T., Bate, M. R., Ogilvie, G. I., & Pringle, J. E. 2002, MNRAS, 337, 967

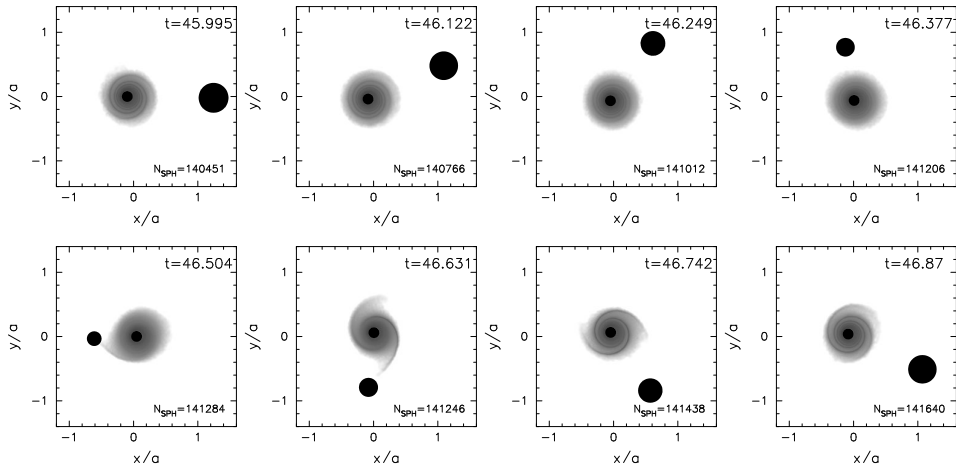


Figure 4. Snapshots covering one orbital period for  $P_{\text{orb}} = 24.3$  d,  $e = 0.34$ , and  $i = 0$ . Each panel shows the logarithm of the surface density. The dark spot near the origin is the Be star, while another dark spot orbiting about the Be star denotes the neutron star with the variable accretion radius.

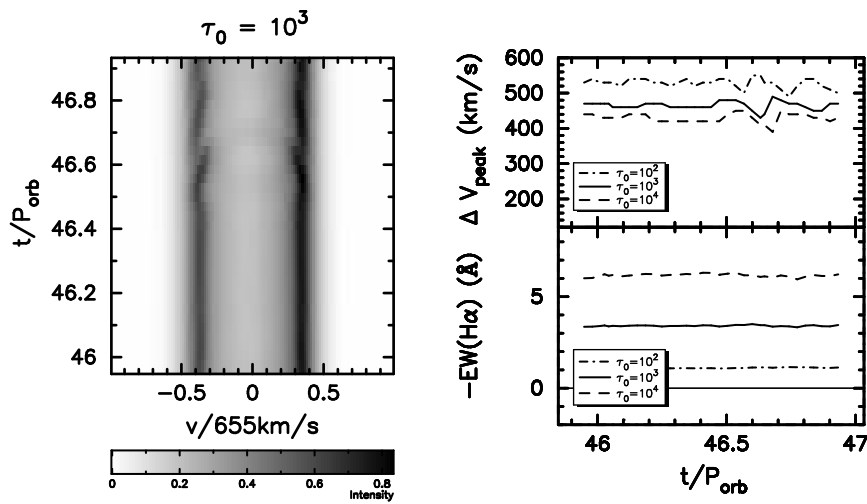


Figure 5. Phase dependence of  $H\alpha$  line profiles for  $P_{\text{orb}} = 24.3$  d,  $e = 0.34$ , and  $i = 0$ . The left panel shows the dynamical spectrum, while the right panels show the orbital modulation in the peak separation (top) and the equivalent width (bottom). In each panel, the dash-dotted line, the solid line, and the dashed line are for the line optical depths of  $10^2$ ,  $10^3$ , and  $10^4$ , respectively.

Porter, J. M. 1999, *A&A*, 348, 512

Reig, P., Fabregat, J. & Coe, M. J. 1997, *A&A*, 322, 193

Zamanov, R. K., Reig, P., Mart, J., Coe, M. J., Fabregat, J., Tomov, N.A., & Valchev, T. 2001, *A&A*, 367, 884